# Optimal Control of Heat and Fluid Flow for Efficient Energy Utilization

**Yosuke Hasegawa**

**Abstract** Application of the optimal control theory to turbulent flows and associated transport phenomena opens up a unique possibility of seeking an optimal set of control inputs (design parameters) without relying on researchers' subjective insights. As an example, it is shown that heat transfer enhancement and skin friction drag reduction is simultaneously achieved in wall turbulence, where it has been considered to be difficult to achieve such dissimilar heat transfer enhancement due to the strong similarity in the governing equations of heat and fluid flow. The control input is assumed to be zero-net-mass-flux wall blowing/suction and its spatio-temporal distribution is optimized so as to minimize a prescribed cost functional defined within a finite time horizon. Surprisingly, the resultant control input exhibits a streamwise traveling wave-like property. Although increase in the time horizon significantly enhances the resultant control performance, time horizons employed in previous studies are commonly limited due to the strong nonlinearity of turbulent flows. Applying a multiple shooting method would be promising to further increase the time horizon, and thereby improve the resultant control performance.

## 1 Background

### *1.1 New Horizon for Optimizing Thermo-Fluids Systems*

Towards achieving the future sustainable society, prediction and control of interfacial phenomena play curtail roles. For example, the turbulent momentum transfer at solid-fluid interfaces governs the energy losses in high-speed transport applications, such as aircrafts, marine vessels, trains, automobiles, pipelines, ventilation systems, to name a few. Enhancing heat and mass transfer across solid-fluid or fluid-fluid interfaces is essential for improving energy efficiencies in air conditioning systems, heat recovery systems, chemical reactors, and so forth. Optimal design

Y. Hasegawa (✉)
Institute of Industrial Science, The University of Tokyo, 4-6-1 Komaba, Meguro-ku, Tokyo 153-8505, Japan
e-mail: ysk@iis.u-tokyo.ac.jp



T. Carraro et al. (eds.), *Multiple Shooting and Time Domain Decomposition Methods*, Contributions in Mathematical and Computational Sciences 9,
DOI 10.1007/978-3-319-23321-5_11

of three-dimensional complex porous structure is particularly important to promote electrochemical reactions in electrodes of solid-oxide fuel cells and lithium ion batteries. Due to the multi-scale and highly non-linear nature of fluid flow and associated transport phenomena, however, optimal design of these energy devices are not trivial. In the present paper, we focus on control of turbulent transport phenomena as a typical example of non-linear problems.

Conventionally, academic researchers have been extracting essential elements from practical problems, and trying to understand the underlying physics. It has been believed that such fundamental knowledge will eventually be useful for designing innovative thermo-fluids systems. Since the first direct numerical simulation (DNS) of wall turbulence by Kim et al. [12], with the aid of rapid development of computational resources, numerical simulation has grown as a powerful tool alternative to existing experimental techniques in deepening our understanding and modeling of complex turbulent transport phenomena. Indeed, the range of application of numerical simulation has been significantly expanded, and this enables to obtain much more detailed flow statistics which cannot be measured experimentally. Despite these progresses, optimization of thermo-fluids systems remain a difficult task. There exists no established approach for predicting how a finite change in a certain design parameter influences resultant drag, heat/mass transfer or chemical reactions in thermo-fluid systems, due to their highly non-linear and multi-scale nature. Optimal control theory opens up a new horizon for seeking an optimal set of design parameters based on the governing equations of underlying physics.

## *1.2 Overview of Turbulence Control Research for Skin Friction Drag Reduction*

During the past several decades, a huge amount of effort of the turbulence research community has been devoted to advance our understanding of turbulent dynamics both experimentally and numerically. Based on this knowledge, various types of control strategies have been proposed. Although flow control has a wide range of applications, such as modifying momentum/heat/mass transfer, suppressing noise, enhancing lift and so forth, we hereafter focus on skin friction drag reduction, which is one of the most active topics in the flow control community.

Existing control schemes are roughly classified into two categories, i.e., active and passive controls. Passive control typified by a riblet surface is advantageous in the sense that it does not require additional energy consumption for flow control. However, their control performance is generally smaller than that of active controls. In addition, they are effective under limited flow conditions close to a design point.

In contrast, active control is generally more flexible and effective, although additional energy consumption for driving actuators is required. Active control is further classified into predetermined and feedback controls. In the former, a

control input with spatio-temporal coherence is specified *a priori* and it is applied without sensing the instantaneous flow field. Starting from spanwise wall oscillation [9], various types of predetermined control schemes have been developed. They are, for example, spanwise traveling wave of body force[5], streamwise traveling wave of wall blowing/suction [14] and deformation [8], standing and traveling waves of spanwise wall forcing [15, 16]. Although significant drag reduction rate is achieved in the predetermined controls, they commonly suffer from relative large energy consumption for applying control. Finding a control input leading to a larger drag reduction rate with smaller control energy input is a major challenge in the predetermined control.

The feedback control generally offers better control performance with small power consumption than the predetermined control. However, it requires a complex sensor-actuator system, possibly fabricated by Micro Electro Mechanical System (MEMS) [10] in order to detect an instantaneous flow state, of which signals are used to trigger actuators. One of the most widely-accepted feed-back control strategy is the so-called opposition control proposed by Choi et al. [4]. In this strategy, wall blowing/suction is applied in order to oppose the wall-normal velocity fluctuation at a certain distance away from the wall. By optimizing the sensing location, they demonstrated 15–20 % drag reduction in DNS of a low Reynolds number turbulent flow. In this study, the control input is determined based on the sensing information inside the fluid domain. In real systems, however, the available information is considered to be limited to wall quantities. Accordingly, Lee et al. [13] developed a control algorithm using wall information based on the suboptimal control theory. In the suboptimal control theory, the control input is optimized so as to minimized a prescribed cost functional in the next computational time step. Their algorithm achieves 12 % drag reduction by using the spanwise wall shear stress or wall pressure. These quantities, however, are in most cases difficult to measure using small sensors distributed on the wall [10]. Hence, Fukagata and Kasagi [6] redefined the cost functional based on the near-wall Reynolds shear stress, and achieve drag reduction by using streamwise wall shear stress, which is the easiest quantity to measure with a relatively small error. In the above studies, the control inputs are optimized by taking into account only short-term dynamics in the suboptimal control framework. The "real" optimal control with a finite, but non-vanishing time horizon was first conducted by Bewley et al. [3], where more than 60 % drag reduction is obtained, and an initial turbulent flow is eventually relaminarized due to the applied control. The significant enhancement of control performance from suboptimal to optimal controls implies the importance of taking into account the future dynamics in determining a control input.

### 1.3 Dissimilar Control of Momentum and Heat Transfer: Less Friction and More Heat Transfer

In many practical problems, one often encounters a significant challenge to not only minimizing drag, but also enhance heat and mass transfer. Indeed, the analysis [2] based on the second law of thermodynamics shows that one of ultimate goals in controlling heat and fluid flow is to achieve an infinitely large heat transfer rate with minimum drag. However, such dissimilar heat transfer enhancement should be a difficult task due to strong similarity between the governing equations of fluid flow and heat in most of shear flows. Namely, on the one hand, turbulence has to be suppressed to reduce drag, but at the same time, mixing has to be promoted in order to enhance heat/mass transfer.

Recently, Kasagi et al. [11] revisited the governing equations and boundary conditions of heat and fluid flow in order to clarify possible scenarios for dissimilar heat transfer control. Among these scenarios, a control strategy based on the fundamental difference between the divergence-free velocity vector and the conservative scalar is considered to be most promising. Based on this idea, Hasegawa and Kasagi [7] first demonstrated dissimilar heat transfer enhancement in a fully developed turbulent channel flow by applying the suboptimal control theory. More recently, Yamamoto et al. [17] applied the optimal control theory to the same problem and higher control performance was obtained. Specifically, they first achieved simultaneous drag reduction and heat transfer enhancement. In the following, we summarize the recent advancement on dissimilar heat transfer enhancement control in wall turbulence.

## 2 Numerical Configurations

### 2.1 Numerical Schemes and Conditions

We consider a fully developed turbulent flow between two parallel plates as shown in Fig. 1. The streamwise, wall-normal and spanwise directions are denoted by $x_1$, $x_2$ and $x_3$, whereas the corresponding velocity components are $u_1$, $u_2$ and $u_3$, respectively. The origin of $x_2$ is located at the center of the channel so that the locations of the two walls are $x_2 = 1$ and $-1$, respectively. The total volume of the computational domain is $V_\Omega$, whereas the domain boundary is expressed by $\Gamma$, the subscript of which represents the normal direction. In all cases, the horizontal channel dimensions are set to $2.5\pi\delta$ and $\pi\delta$ in $x_1$ and $x_3$ directions, respectively. These are sufficiently large to reproduce the reliable turbulent statistics in a low Reynolds number flow considered here.

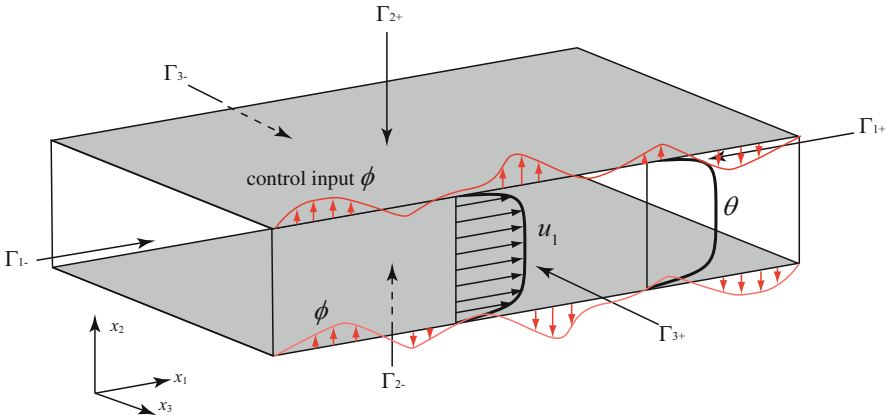


**Fig. 1** Computational domain and coordinate system

The governing equations of incompressible fluid flow are given by the following Navier-Stokes and continuity equations:

$$\frac{\partial u_i}{\partial t} + u_j \frac{\partial u_i}{\partial x_j} = -\frac{\partial p}{\partial x_i} + \frac{1}{Re} \frac{\partial^2 u_i}{\partial x_j \partial x_j}, \tag{1}$$

$$\frac{\partial u_i}{\partial x_i} = 0. \tag{2}$$

Here, all variables are normalized by the bulk mean velocity $U_b$ defined later in Eq. (7) and the channel half depth $\delta$, so that the dimensionless channel height is two (see, Fig. 1), whereas $p$ is the static pressure and $t$ is time. The Reynolds number is defined as $Re = U_b \delta / \nu$, where $\nu$ is the kinematic viscosity of fluid.

The temperature is treated as a passive scalar, so that any buoyancy effects do not arise. Consequently, the transport equation of heat is given by

$$\frac{\partial \theta}{\partial t} + u_j \frac{\partial \theta}{\partial x_j} = Q + \frac{1}{PrRe} \frac{\partial^2 \theta}{\partial x_j \partial x_j}. \tag{3}$$

Here, the temperature is also non-dimensionalized by the temperature difference between the bulk fluid and the wall, $\Theta_b - \Theta_w$. The Prandtl number is the ratio of $\nu$ and the thermal diffusivity $\alpha$, i.e., $Pr = \nu/\alpha$, whilst the heat source term $Q$ is generally a function of time and space.

In the present study, the heat source is assumed to be time-independent and spatially uniform throughout the computational domain, and identical to the mean pressure gradient:

$$Q = -\overline{\frac{\partial p}{\partial x_1}}, \tag{4}$$

where the over-bar represents averaging in the homogeneous directions, i.e., $x_1$ and $x_3$, and also time $t$. In addition, $Pr$ is also set to be unity. This particular condition is chosen, since it makes the transport equations and boundary conditions for $u_1$ and $\theta$ similar, so that the essential difference between the divergence-free velocity vector and the conservative scalar can be analyzed[7]. We also note that the present ideal condition is close to the thermal conditions in real heat exchangers[17].

We consider local wall blowing/suction with zero-net-mass-flux as a control input. For the tangential velocity components and the temperature, we impose the no-slip and constant-temperature conditions at two walls. The resultant wall boundary conditions are described as

$$u_i\Big|_{\Gamma_{2\pm}} = \phi n_i, \tag{5}$$

$$\theta\Big|_{\Gamma_{2\pm}} = 0. \tag{6}$$

Here, the control input, i.e., the wall-normal velocity component imposed at the wall, is denoted by $\phi$, the sign of which is defined to be positive when the applied control input is directed to the outer normal vector $n_i$ at the boundaries of the fluid domain. In the horizontal directions $x_1$ and $x_3$, we apply periodic boundary conditions.

The governing equations (1)–(3) for the velocity and thermal fields are solved by DNS with a second-order finite volume method. More detailed description of the numerical scheme can be found in Yamamoto et al. [17]. All calculations are conducted under a constant bulk mean velocity and the Reynolds number is mostly set to be $\mathrm{Re} = 2293$. Due to the similarity in the mathematical form between physical and adjoint problems (see, Eqs. (16) and (23)), the essentially same numerical method is used for solving the adjoint velocity and thermal fields introduced later.

## 2.2 Control Performance Indices

Following Hasegawa and Kasagi [7], the bulk velocity $U_b$ and the bulk temperature $\Theta_b$ are respectively defined as the following cross-sectional average of flow rate and temperature:

$$U_b = \frac{1}{V_\Omega}\int_\Omega u_1 dV, \tag{7}$$

$$\Theta_b = \frac{1}{V_\Omega}\int_\Omega \theta dV. \tag{8}$$

As the indices of heat transfer and pressure loss, the following Stanton number $St$ and the friction coefficient $C_f$ are defined:

$$St = \frac{q_w}{U_b(\Theta_b - \Theta_w)}, \tag{9}$$

$$C_f = \frac{\tau_w}{\frac{1}{2}{U_b}^2}, \tag{10}$$

where

$$q_w = -\frac{1}{PrRe}\frac{\partial\overline{\theta}}{\partial y}n_2\Big|_{\Gamma_2}, \tag{11}$$

$$\tau_w = -\frac{1}{Re}\frac{\partial\overline{u_1}}{\partial y}n_2\Big|_{\Gamma_2} \tag{12}$$

are the dimensionless wall heat flux and skin friction, respectively.

If the profiles of the averaged streamwise velocity and temperature are similar, $2St$ is exactly equal to $C_f$ at $Pr = 1$. Therefore, we define an analogy factor as

$$A = \frac{2\mathrm{St}}{C_f}. \tag{13}$$

Physically, $A$ represents heat transfer per unit pumping power. The main objective in dissimilar control is to increase $A$ from unity by manipulating turbulence.

## 2.3 Optimization Procedure

In applying optimal control theory to flow problems, a cost functional is first defined, and then a control input is iteratively updated so as to minimize the cost function within a prescribed time horizon. The correction of a control input in each iteration is obtained by solving the adjoint velocity and thermal fields backward in time. Ideally, the time horizon should be long enough to cover the whole life-time of turbulence dynamics, but it is not computationally trackable. Therefore, it is common to choose an intermediate finite time horizon $T$ as shown in Fig. 2. Once a control input converges, the time horizon is advanced by $T_a$, and then a new optimization procedure in the next time horizon starts. In the following, we define the cost functional, derive the adjoint equations, and describe the optimization procedures without getting into the mathematical details, which can be found in other literatures [1, 3]. In the present study, the time horizon is set to be $T/(\delta/U_b) = 10$, which is almost identical to the maximal value used in the drag reduction control by Bewley et al. [3], while $T_a = T/10$ is employed.

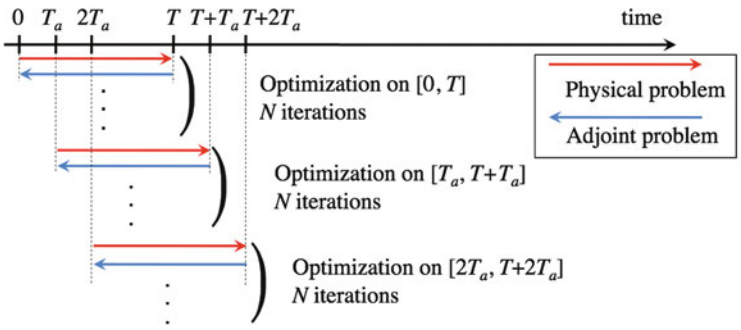


**Fig. 2** Schematic of optimization procedure. In each time horizon, the evolution of velocity and thermal fields are solved under a preliminary control input as shown by the *red arrows*, which is followed by adjoint computation depicted by the *blue arrows*

### 2.3.1 Defining the Cost Functional

We define a cost functional as follows:

$$\begin{aligned} J &= \kappa \int_0^T \int_{\Gamma_{2\pm}} \frac{1}{2}\phi^2 dSdt - A \\ &\approx \kappa \int_0^T \int_{\Gamma_{2\pm}} \frac{1}{2}\phi^2 dSdt - \frac{\displaystyle\int_0^T \int_{\Gamma_{2\pm}} -\frac{1}{PrRe}\frac{\partial\theta}{\partial n} dSdt}{\displaystyle\int_0^T \int_{\Gamma_{2\pm}} -\frac{1}{Re}\frac{\partial u}{\partial n} dSdt}, \end{aligned} \tag{14}$$

where $t = 0$ corresponds to the beginning of the time horizon. The first term represents the cost of control, while the second term is exactly a quantity we attempt to enhance, i.e., the analogy factor. Hence, under this cost functional, the control input is optimized so as to maximize $A$ with the least intensity of wall blowing/suction. Ideally, $A$ has to be determined by the ratio of $2St$ and $C_f$ integrated over a sufficiently long period. Since the optimal control theory takes into account only flow dynamics within a finite time horizon, however, $A$ is approximated by the integrals within the time horizon as shown in the second line of Eq. (14). The weight coefficient $\kappa$ corresponds to the relative cost of the control input. In the present study, $\kappa$ is specified so that the intensity of the control input $\phi$ is 5 % of the bulk mean velocity.

### 2.3.2 Optimal Control Theory

For ease of notation, the flow state $\boldsymbol{\psi}$, the flow perturbation state $\boldsymbol{\psi}'$ and the adjoint state $\boldsymbol{\psi}^*$ are expressed as the following vector forms:

$$\boldsymbol{\psi} = \begin{pmatrix} p \\ u_i \\ \theta \end{pmatrix}, \boldsymbol{\psi}' = \begin{pmatrix} p' \\ u_i' \\ \theta' \end{pmatrix}, \boldsymbol{\psi}^* = \begin{pmatrix} p^* \\ u_i^* \\ \theta^* \end{pmatrix}. \tag{15}$$

The governing equations (1)–(3) for the velocity and thermal fields can be written in a functional form as

$$N(\boldsymbol{\psi}) = \begin{pmatrix} \dfrac{\partial u_i}{\partial x_i} \\ \dfrac{\partial u_i}{\partial t} + \dfrac{\partial u_j u_i}{\partial x_j} - \dfrac{1}{\mathrm{Re}} \dfrac{\partial^2 u_i}{\partial x_j{}^2} + \dfrac{\partial p}{\partial x_i} \\ \dfrac{\partial \theta}{\partial t} + \dfrac{\partial u_j \theta}{\partial x_j} - \dfrac{1}{\mathrm{RePr}} \dfrac{\partial^2 \theta}{\partial x_j^2} - Q \end{pmatrix} = \mathbf{0}. \tag{16}$$

Then, we consider the perturbation field $\boldsymbol{\psi}'$ of velocity and thermal fields induced by a small change of a control input $\phi$. Following Bewley et al. [3], the perturbation is defined by the Frechét differential of the original flow state $\boldsymbol{\psi}$ as

$$\boldsymbol{\psi'} \triangleq \lim_{\epsilon \to 0} \frac{\boldsymbol{\psi}(\phi + \phi' \epsilon) - \boldsymbol{\psi}(\phi)}{\epsilon}, \tag{17}$$

where $\epsilon$ is an infinitesimal constant.

Since both the original and perturbed flow states satisfy Eq. (16), the following linear equations for $\boldsymbol{\psi'}$ is obtained:

$$N'(\boldsymbol{\psi'}) = \begin{pmatrix} \dfrac{\partial u_i'}{\partial x_i} \\ \dfrac{\partial u_i'}{\partial t} + \dfrac{\partial}{\partial x_j}\left(u_j u_i' + u_j' u_i\right) - \dfrac{1}{\mathrm{Re}} \dfrac{\partial^2 u_i'}{\partial x_j{}^2} + \dfrac{\partial p'}{\partial x_i} \\ \dfrac{\partial \theta'}{\partial t} + \dfrac{\partial}{\partial x_j}\left(u_j \theta' + u_j' \theta\right) - \dfrac{1}{\mathrm{RePr}} \dfrac{\partial^2 \theta'}{\partial x_j^2} \end{pmatrix} = \mathbf{0}, \tag{18}$$

where the wall boundary conditions are given by

$$u_i' = -\phi' n_i, \ \theta' = 0 \quad \text{on } \Gamma_{\pm 2}, \tag{19}$$

$$u_i' = \mathbf{0}, \ \theta' = 0 \quad \text{at } t = 0. \tag{20}$$

In Eq. (18), the products between perturbations are all neglected since the perturbation is assumed to be sufficiently small. Although Eqs. (18)–(20) indicate the linear relationship between $\phi'$ and $\boldsymbol{\psi}'$, it is not straightforward to derive the explicit relationship between $\phi'$ and the resultant change of the cost functional $J'$. In order to overcome this difficulty, the adjoint velocity and thermal fields are introduced.

The flow optimization can generally be viewed as a minimization problem of a cost functional $J$ under the constraints on the flow states, i.e., the governing equations and the boundary conditions of flow and thermal fields. This is equivalent to minimizing the following Hamiltonian $H$:

$$H = J - \langle N(\boldsymbol{\psi}), \boldsymbol{\psi}^* \rangle , \tag{21}$$

where the adjoint state $\boldsymbol{\psi}^*$ corresponds to the Lagrangian multiplier.

The Frechét differential of Eq. (21) leads to

$$\begin{aligned} \frac{\mathscr{D}H}{\mathscr{D}\phi}\phi' &= J' - \left\langle N'(\boldsymbol{\psi}'), \boldsymbol{\psi}^* \right\rangle \\ &= J' - \left\langle \boldsymbol{\psi}', N^*(\boldsymbol{\psi}^*) \right\rangle - b, \end{aligned} \tag{22}$$

where $N^*$ is the adjoint operator of $N'$. We impose the following relationship for the adjoint field:

$$N^*(\boldsymbol{\psi}^*) = \begin{pmatrix} -\dfrac{\partial u_i^*}{\partial x_i} \\ -\dfrac{\partial u_i^*}{\partial t} - u_j\left(\dfrac{\partial u_i^*}{\partial x_j} + \dfrac{\partial u_j^*}{\partial x_i}\right) - \dfrac{1}{\mathrm{Re}}\dfrac{\partial^2 u_i^*}{\partial x_j{}^2} - \dfrac{\partial p^*}{\partial x_i} - \theta\dfrac{\partial \theta^*}{\partial x_i} \\ -\dfrac{\partial \theta^*}{\partial t} - u_j\dfrac{\partial \theta^*}{\partial x_j} - \dfrac{1}{\mathrm{RePr}}\dfrac{\partial^2 \theta^*}{\partial x_j^2} \end{pmatrix} = \mathbf{0}, \tag{23}$$

so that the second term on the right-hand-side of Eq. (22) vanishes. The first term on the right-hand-side of Eq. (22) is the Frechét differential of the cost functional, and can be written as

$$\begin{aligned} J' = {} & \kappa \int_0^T \int_{\Gamma_{2\pm}} \phi\phi' dSdt \\ & + \frac{A}{TS_{\Gamma_{2\pm}}\tau_w}\int_0^T \int_{\Gamma_{2\pm}} -\frac{\partial u'}{\partial n} dSdt - \frac{A}{TS_{\Gamma_{2\pm}}q_w}\int_0^T \int_{\Gamma_{2\pm}} -\frac{\partial \theta'}{\partial n} dSdt, \end{aligned} \tag{24}$$

where $S_{\Gamma 2\pm}$ represents the boundary area of $\Gamma_{2\pm}$. The third term on the right-hand-side of Eq. (22) is called a boundary term, since it includes only boundary integrals

as shown below:

$$b = \int_{\Omega} (u_j' u_j^* + \theta' \theta^*)\Big|_{t+=0}^{t+=T} dV$$
$$+ \int_0^T \int_{\Gamma_{2\pm}} n_j \Big[ p^* u_j' + u_j^* p' + u_i^* (u_j u_i' + u_i u_j') - \frac{1}{\mathrm{Re}} (u_i^* \frac{\partial u_i'}{\partial x_j} - u_i' \frac{\partial u_i^*}{\partial x_j})$$
$$+ (u_j' \theta + u_j \theta') \theta^* - \frac{1}{\mathrm{RePr}} (\theta^* \frac{\partial \theta'}{\partial x_j} - \theta' \frac{\partial \theta^*}{\partial x_j}) \Big] dS dt. \tag{25}$$

The terminal and boundary conditions for the adjoint state are given by

$$\boldsymbol{\psi}^*\Big|_{t=T} = \mathbf{0} \tag{26}$$
$$u_i^*\Big|_{\Gamma_{2\pm}} = A \frac{\mathrm{Re}}{TS_{\Gamma_{2\pm}} \tau_w} \delta_{1i} \tag{27}$$
$$\theta^*\Big|_{\Gamma_{2\pm}} = -A \frac{\mathrm{RePr}}{TS_{\Gamma_{2\pm}} q_w}, \tag{28}$$

so that the integrand of Eq. (22) is eventually factorized by $\phi'$ as follows

$$\frac{\mathscr{D}H}{\mathscr{D}\phi} \phi' = J' - \left\langle \boldsymbol{\psi}', N^*(\boldsymbol{\psi}^*) \right\rangle - b$$
$$= \kappa \int_0^T \int_{\Gamma_{2\pm}} \phi \phi' dS dt - \frac{A}{\tau_w} \int_0^T \int_{\Gamma_{2\pm}} \frac{\partial u'}{\partial n} dS dt + \frac{A}{q_w} \int_0^T \int_{\Gamma_{2\pm}} \frac{\partial \theta'}{\partial n} dS dt$$
$$- \int_0^T \int_{\Gamma_{2\pm}} \Big[ p^* \phi' - \frac{A}{\tau_w} \frac{\partial u_i'}{\partial n} + \frac{A}{q_w} \frac{\partial \theta'}{\partial n} \Big] dS dt$$
$$= \int_0^T \int_{\Gamma_{2\pm}} \left( \kappa \phi - p^* \right) \phi' dS dt. \tag{29}$$

The final form of Eq. (29) guarantees that correcting the control input by $\phi' = -(\kappa\phi - p^*)$ decreases $H$. Therefore, after solving the adjoint field, the control input is updated as follows:

$$\phi^{n+1} = \phi^n - \beta(\kappa \phi^n - p^*), \tag{30}$$

where the superscript represents the number of iteration, while $\beta$ is a relaxation coefficient. In the present study, $\beta$ is determined so that both $|\phi^{n+1} - \phi^n| < 3.0 \times 10^{-3}$. This increases $\beta$ as the control input converges. Hence, $\beta < 8$ is also imposed throughout the optimization procedure.

### 2.3.3 Suboptimal Control Theory

One of major obstacles in applying the optimal control theory to fluid flow and associated transport phenomena is to solve physical and adjoint problems iteratively within a time horizon as shown in Fig. 2. In addition, solving the adjoint equations requires complete information of the physical field during the time horizon (see, Eq. (23)), so that large memory capacity is needed. In order to mitigate the computational load, the suboptimal control theory was developed. In the suboptimal control, a control input minimizing a cost functional within a vanishingly small time horizon is considered. Neglecting the response of the non-linear terms appearing in Eqs. (1)–(3) to an infinitesimal change of control input, the short-term response of the velocity and thermal fields to a control input can be obtained analytically by taking into account linear processes only.

The suboptimal control input for dissimilar heat transfer enhancement was derived in Hasegawa and Kasagi [7]. The resultant control inputs at bottom and top walls are given by

$$\hat{\phi}\Big|_{\Gamma_{2-}} = \gamma\left[\int_{-1}^{1} y\left\{\frac{\sinh\{k(y-1)\}}{\sinh(2k)}\hat{u}_1(y) - \frac{ik_1\cosh\{k(y-1)\}}{k\cdot\sinh(2k)}\hat{u}_2(y)\right\}dy - \int_{-1}^{1} y\left\{\frac{\sinh\{k(y-1)\}}{\sinh(2k)}\hat{\theta}(y)\right\}dy\right], \tag{31}$$

$$\hat{\phi}\Big|_{\Gamma_{2+}} = \gamma\left[\int_{-1}^{1} y\left\{-\frac{\sinh\{k(y+1)\}}{\sinh(2k)}\hat{u}_1(y) + \frac{ik_1\cosh\{k(y+1)\}}{k\cdot\sinh(2k)}\hat{u}_2(y)\right\}dy + \int_{-1}^{1} y\left\{\frac{\sinh\{k(y+1)\}}{\sinh(2k)}\hat{\theta}(y)\right\}dy\right]. \tag{32}$$

Here, $\hat{\cdot}$ represents Fourier coefficient for a particular combination of the streamwise and spanwise wave numbers, i.e., $k_x$ and $k_z$, and $k = \sqrt{k_x^2 + k_z^2}$. It should be emphasized that the control inputs (31), (32) are expressed with the information of the physical field at the same instant. Therefore, the iterative computation of the adjoint field is not required in the suboptimal control.

The proportional constant $\gamma$ is determined so that the intensity of $\phi$ is equal to 5 % of the bulk mean velocity as is the case for the optimal control introduced in the previous subsection.

## 3 Results

In this section, the control performances achieved by the optimal and suboptimal control theories are compared. Note that the control performance is generally

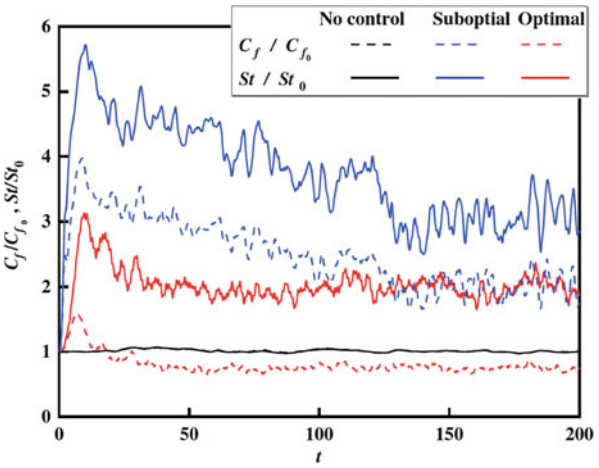


**Fig. 3** Time traces of $C_f$ and $St$ achieved in the optimal and suboptimal controls normalized by the values of the uncontrolled flow

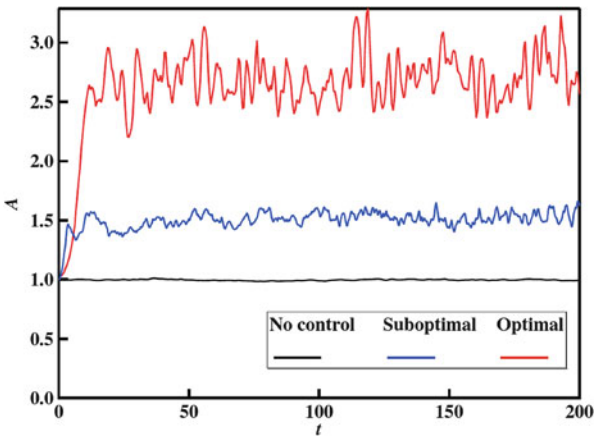


**Fig. 4** Time traces of analogy factor achieved in the optimal and suboptimal controls

enhanced with increasing the intensity of the control input. Accordingly, the intensity of the control input is fixed to 5 % of the bulk mean velocity in both controls for fair comparison.

In Fig. 3, the time traces of $C_f$ and $St$ obtained in the suboptimal and optimal controls normalized by the values in the uncontrolled flow are shown. In the case of the suboptimal control, $C_f$ and $St$ are both increased due to the control. However, $St$ is enhanced more than $C_f$. Specifically, $St$ is increased three times from the uncontrolled value, whereas $C_f$ remains only doubled. In the case of optimal control, more significant control performance can be confirmed. Namely, $St$ is doubled, whilst $C_f$ is decreased by 30 % from the uncontrolled value. This is a surprising result, since 30 % drag reduction rate is larger than that obtained in the opposition control [4]. In addition, the opposition control causes drag reduction only, but does not enhance heat transfer. The time trace of the analogy factor $A$ is shown in Fig. 4.

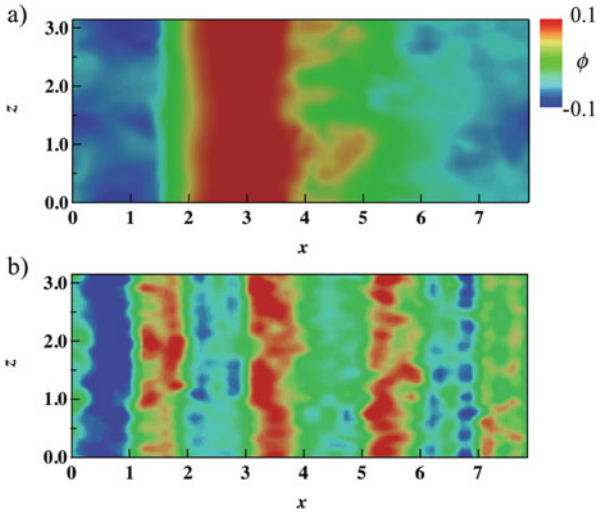


**Fig. 5** Instantaneous snapshot of the control input obtained in (**a**) suboptimal and (**b**) optimal control theories. The flow direction is from left to right

It is found that $A \approx 1.5$ is achieved in the suboptimal control, whereas $A$ reaches as high as 2.7 in the optimal control.

The top views of the instantaneous control inputs at the bottom wall obtained in the suboptimal and optimal control theories are shown in Fig. 5. The red and blue colors correspond to regions of wall blowing and suction, respectively. Interestingly, both the control inputs are characterized by wavy distributions in the streamwise direction. In addition, visualization of time traces of these waves (not shown here) reveals that they travel downstream at a constant phase speed, which is around 20–30 % of the bulk mean velocity [7, 17]. These results indicate that the streamwise traveling wave of wall blowing/suction is promising for enhancing heat transfer with minimum pressure penalty.

## 4 Discussions: Possible Application of Multiple Shooting Method

The advantage of applying the optimal control theory to flow problems is that a control input is optimized based on the governing equations of heat and fluid flow. As shown in Fig. 5, the present control inputs obtained by the optimal and suboptimal control theories commonly exhibit a streamwise traveling-wave like property. Despite their simplicity, it is quite difficult to derive such a control strategy only from researchers' physical insight.

It is also interesting to compare the control performances obtained in the suboptimal and optimal control theories. Obviously, the control performance achieved in the optimal control theory with a finite time horizon $T$ is better than that achieved in

the suboptimal control theory, where a vanishingly small time horizon is assumed. Similar trend is also observed in the drag reduction control by Bewley et al. [3].

Although there is tendency that a larger $T$ results in better control performance up to $T \approx 10$, it is found that further increase of the time horizon makes the adjoint computation diverge. This could be attributed to the fact that the mathematical derivation of the optimal control input is based on the linearized perturbation equation (18), where the perturbation of a flow state induced by a small change of a control input is assumed to remain sufficiently small during the time horizon, so that all non-linear terms can be neglected. However, it is well-known that a small disturbance grows very rapidly in turbulent flow due to its nonlinear nature. This implies that the perturbation equation (18) is invalid for a large time horizon. Obviously, a different approach is necessary to extend the time horizon further. In this respect, a multiple shooting technique would be an interesting option. Its application to flow problems remains the future work.

## 5 Summary

Although significant progresses have been made in understanding and modeling turbulent flows in the last few decades, control of turbulence and associated transport phenomena remains a challenging task due to their highly nonlinear and multi-scale nature. The optimal control theory provides a unique opportunity to optimize a control input without relying on researchers' subjective insights. In the present article, we apply two different approaches, i.e., the optimal and suboptimal control theories, to wall turbulence with heat transfer. In the former, the control input is determined so as to minimize a prescribed cost functional defined within a finite time horizon, whereas in the latter, the time horizon is assumed to be infinitesimal, so that the response of the non-linear terms are all neglected. Although the suboptimal control theory has advantage that it does not require iterative computations of the physical and adjoint equations, there exists a general trend that the control performance is enhanced with increasing the time horizon. This implies significance of taking into consideration the future dynamics in determining the control input. However, the time horizons employed in previous studies are commonly limited due to strong non-linearity of turbulent flows. Applying a multiple shooting method would be one promising option for further increasing the time horizon, and thereby achieving higher control performances.

## References

1. Abergel, F., Temam, R.: On some control problems in fluid mechanics. Theor. Comput. Fluid Dyn. **1**, 303–325 (1990)
2. Bejan, A.E.: General criterion for rating heat-exchanger performance. Int. J. Heat Mass Transfer **21**, 655–658 (1978)

3. Bewley, T., Moin, P., Temam, R.: DNS-based predictive control of turbulence: an optimal benchmark for feedback algorithms. J. Fluid Mech. **447**, 179–225 (2001)
4. Choi, H., Moin, P., Kim, J.: Active turbulence control for drag reductio in wall-bounded flows. J. Fluid Mech. **262**, 75–110 (1994)
5. Du, Y., Karniadakis, G.: Suppressing wall turbulence by means of a transverse traveling wave. Science **288**, 1230 (2000)
6. Fukagata, K., Kasagi, N.: Suboptimal control for drag reduction via suppression of near-wall Reynolds shear stress. Int. J. Heat Fluid Flow **25**, 341—350 (2004)
7. Hasegawa, Y., Kasagi, N.: Dissimilar control of momentum and heat transfer in a fully developed turbulent channel flow. J. Fluid Mech. **683**, 57–93 (2011)
8. Hoepffner, J., Fukagata, K.: Pumping or drag reduction? J. Fluid Mech. **635**, 171–187 (2009)
9. Jung, W., Mangiavacchi, N., Akhavan, R.: Suppression of turbulence in wall-bounded flows by high-frequency spanwise oscillation. Phys. Fluids A **4**, 1605–1607 (1992)
10. Kasagi, N., Suzuki, Y., Fukagata, K.: Microelectromechanical systems-based feedback control of turbulence for skin friction reduction. Annu. Rev. Fluid Mech. **41**, 231–251 (2009)
11. Kasagi, N., Hasegawa, Y., Fukagata, K., Iwamoto, K.: Control of turbulent transport: less friction and more heat transfer. Trans. ASME J. Heat Transf. **134**, 031009 (2012)
12. Kim, J., Moin, P., Moser, R.: Turbulent statistics in fully developed channel flow at a low Reynolds number. J. Fluid Mech. **177**, 133–166 (1987)
13. Lee, C., Kim, J., Choi, H.: Suboptimal control of turbulent channel flow for drag reduction. J. Fluid Mech. **358**, 245–258 (1998)
14. Min, T., Kang, J., Kim, J.: Sustained sub-laminar drag in a fully developed channel flow. J. Fluid Mech. **558**, 309–318 (2006)
15. Quadrio, M., Ricco, P., Viotti, C.: Streamwise-travelling waves of spanwise wall velocity for turbulent drag reduction. J. Fluid Mech. **627**, 161–178 (2009)
16. Viotti, C., Quadrio, M., Luchini, P.: Streamwise oscillation of spanwise velocity at the wall of a channel for turbulent drag reduction. Phys. Fluids **21**, 115109 (2009)
17. Yamamoto, A., Hasegawa, Y., Kasagi, N.: Optimal control of dissimilar heat and momentum transfer in a fully developed turbulent channel flow. J. Fluid Mech. **733**, 189–220 (2013)